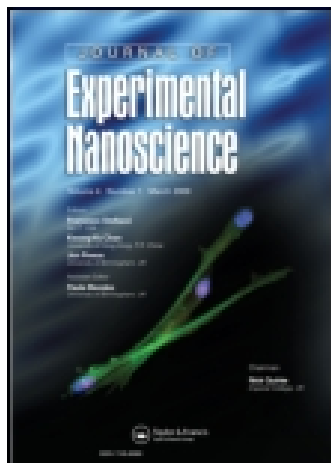


This article was downloaded by: [Korea Advanced Institute of Science & Technology (KAIST)]

On: 21 January 2015, At: 21:35

Publisher: Taylor & Francis

Informa Ltd Registered in England and Wales Registered Number: 1072954 Registered office: Mortimer House, 37-41 Mortimer Street, London W1T 3JH, UK



Journal of Experimental Nanoscience

Publication details, including instructions for authors and subscription information:

<http://www.tandfonline.com/loi/tjen20>

Microstructure and mechanical properties of CNT/Ag nanocomposites fabricated by spark plasma sintering

Walid M. Daoush^a, Byung K. Lim^b, Dong H. Nam^b & Soon H. Hong^b

^a Department of Powder Technology at Central Metallurgical Research & Development Institute, Cairo, Egypt

^b Department of Materials Science and Engineering, Korea Advanced Institute of Science and Technology, 373-1 Guseong-dong, Yuseong-gu, Daejeon 305-701, Korea

Published online: 11 Jul 2012.



CrossMark

[Click for updates](#)

To cite this article: Walid M. Daoush, Byung K. Lim, Dong H. Nam & Soon H. Hong (2014) Microstructure and mechanical properties of CNT/Ag nanocomposites fabricated by spark plasma sintering, Journal of Experimental Nanoscience, 9:6, 588-596, DOI: [10.1080/17458080.2012.680927](https://doi.org/10.1080/17458080.2012.680927)

To link to this article: <http://dx.doi.org/10.1080/17458080.2012.680927>

PLEASE SCROLL DOWN FOR ARTICLE

Taylor & Francis makes every effort to ensure the accuracy of all the information (the "Content") contained in the publications on our platform. However, Taylor & Francis, our agents, and our licensors make no representations or warranties whatsoever as to the accuracy, completeness, or suitability for any purpose of the Content. Any opinions and views expressed in this publication are the opinions and views of the authors, and are not the views of or endorsed by Taylor & Francis. The accuracy of the Content should not be relied upon and should be independently verified with primary sources of information. Taylor and Francis shall not be liable for any losses, actions, claims, proceedings, demands, costs, expenses, damages, and other liabilities whatsoever or howsoever caused arising directly or indirectly in connection with, in relation to or arising out of the use of the Content.

This article may be used for research, teaching, and private study purposes. Any substantial or systematic reproduction, redistribution, reselling, loan, sub-licensing, systematic supply, or distribution in any form to anyone is expressly forbidden. Terms &

Conditions of access and use can be found at <http://www.tandfonline.com/page/terms-and-conditions>

Microstructure and mechanical properties of CNT/Ag nanocomposites fabricated by spark plasma sintering

Walid M. Daoush^{a*†}, Byung K. Lim^b, Dong H. Nam^b and Soon H. Hong^b

^aDepartment of Powder Technology at Central Metallurgical Research & Development Institute, Cairo, Egypt; ^bDepartment of Materials Science and Engineering, Korea Advanced Institute of Science and Technology, 373-1 Guseong-dong, Yuseong-gu, Daejeon 305-701, Korea

(Received 6 September 2011; final version received 23 March 2012)

Carbon nanotube/silver (CNT/Ag) nanocomposites include CNT volume fraction up to 10 vol.% were prepared by chemical reduction in solution followed by spark plasma sintering. Multiwalled CNTs underwent surface modifications by acid treatments, the Fourier transform infrared spectroscopy data indicated several functional groups loaded on the CNT surface by acid functionalisation. The acid-treated CNTs were sensitised and activated. Silver was deposited on the surface of the activated CNTs by chemical reduction of alkaline silver nitrate solution at room temperature. The microstructures of the prepared CNT/Ag nanocomposite powders were investigated by high-resolution scanning electron microscopy (HRSEM), transmission electron microscopy and X-ray powder diffraction analysis. The results indicated that the produced CNT/Ag nanocomposite powders have coated type morphology. The produced CNT/Ag nanocomposite powders were sintered by spark plasma sintering. It was observed from the microstructure investigations of the sintered materials by HRSEM that the CNTs were distributed in the silver matrix with good homogeneity. The hardness and the tensile properties of the produced CNT/Ag nanocomposites were measured. By increasing the volume fraction of CNTs in the silver matrix, the hardness values increased but the elongation values of the prepared CNT/Ag nanocomposites decreased. In addition, the tensile strength was increased by increasing the CNTs volume fraction up to 7.5 vol.%, but the sample composed of 10 vol.% CNT/Ag was fractured before yielding.

Keywords: multiwalled carbon nanotube; silver deposition; spark plasma sintering; hardness; tensile properties

1. Introduction

Since carbon nanotubes (CNTs) were discovered, great studies have been made in exploiting their properties [1,2]. Theoretical and experimental studies have shown that these materials possess both excellent mechanical properties, such as elastic moduli as high as 1 TPa and strengths from 10 to 100 times higher than the strongest steel at a fraction of the weight, excellent toughness and superior physical properties, such as thermal conductivity about twice as high as diamond and electric current-carrying capacity 1000 times higher than copper wires [3,4]. Because of these excellent properties, CNTs are considered the ideal type of fibre-like reinforcements for fabrications of composite materials especially electrical contact materials instead of graphite and carbon fibre [5–7].

*Corresponding author. Email: waleeddaush@cmrdi.sci.eg

†Present address: Department of Production Technology, Helwan University, Cairo, Egypt.

The primary function of electrical contact materials is to carry current and to break it [8,9]. Silver-graphite composites are typical electrical contact materials. Graphite has its deficiencies including brittleness, low strength, and current-carrying capacity [10]. It is supposed that silver reinforced with CNTs would have better properties than graphite or carbon fibre. As with carbon fibre-reinforced metal matrix composites, the performance of the CNTs-reinforced metal matrix composites is largely controlled by the interface between the nanotubes and the metal matrix. In general, the metal matrix poorly wets the CNTs so that the interface of CNTs with silver is extremely weak.

In case of electrical brush-rotor systems composed of silver-graphite composites [11], the currents pass between a brush and a rotor that slide against each other and both the brush and slip ring experience wear. As the brush material is softer than that of the slip ring, the brushes wear out first. Excessive wear rate has been observed for silver-graphite brushes due to the combined effects of the high current density and the high sliding speed. It is desirable for the brush to operate with minimum mechanical loss (low coefficient of friction), minimum electrical loss (low contact resistance at the sliding interface) and long brush life (low rate of wear) [12,13]. As CNTs have excellent mechanical and physical properties and low density as well as good wear and friction properties, CNTs offer tremendous opportunities for the development of fundamentally new material system for electric contact material applications [14,15]. Recently, preliminary research in nanotube-based composite has been carried out on polymer- or ceramic-matrix materials to improve their mechanical properties (such as the elastic modulus, yield strength and fracture toughness) [16,17].

Carbon nanotube has similar properties like graphite such as low wettability to metals. In order to use CNTs as a reinforcement dispersed in composite matrix, it must undergo surface treatments to increase the interaction between CNTs and metal matrix [18–22]. Coating techniques is one of the techniques that has been used to increase the interaction between the metal matrix and CNTs. After which, the coated layers can serve as medium for adhesion and transferring loads.

This work aims to improve the distribution of CNTs in silver matrix by depositing silver on the CNTs surfaces to produce CNT/silver (Ag) nanocomposite powders with different CNTs volume fraction. The produced CNT/Ag nanocomposite powders were sintered by spark plasma sintering technique. The microstructures of the sintered materials were investigated by scanning electron microscopy (SEM) and transmission electron microscopy (TEM) as well as X-ray powder diffraction (XRD). The hardness and the tensile properties of the produced materials were measured.

2. Experimental

Multiwalled CNT grade of 10–50 μm length and 10–15 nm diameter with Brunauer, Emmett, and Teller (BET) surface area about 200 m^2/g was supplied from Iljin Nanotech Co., Ltd. Highly pure concentrated hydrochloric, nitric and sulphuric acids were used for acid-treating of CNTs by surface oxidation process as mentioned in our previous work [23].

The acid-treated CNTs underwent sensitisation and silver depositions on its surfaces. The silver deposition bath was composed of highly pure chemicals of stannous chloride dihydrate, silver nitrate; ammonia solution and formaldehyde were supplied from Aldrich Co., Germany. Stannous chloride aqueous solution of 2 wt.% was used to sensitise the acid-treated CNTs by magnetic stirring at 500 rpm for 24 h, and the pH of the solution was adjusted between 1 and 3 using hydrochloric acid. The sensitised CNTs underwent washing with distilled water, centrifugation and filtration followed by catalytic treatment by magnetic stirring at 500 rpm in silver nitrate solution for 2 h. The pH of the solution was adjusted around 9 at room

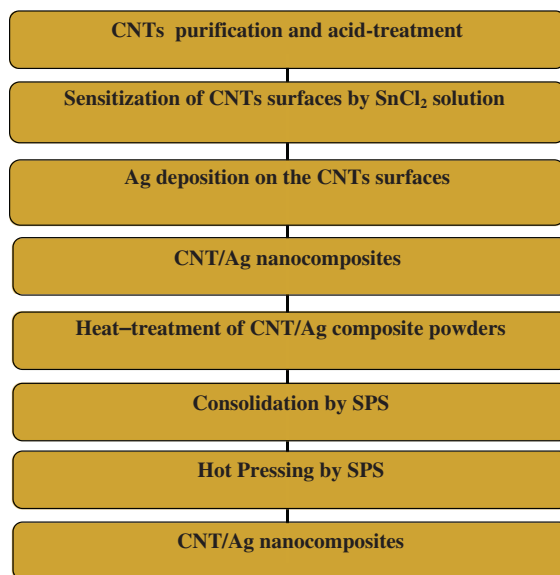


Figure 1. Schematic fabrication process steps of CNT/Ag nanocomposites.

temperature. When the reduction reaction of the silver deposition is completed, the CNT/Ag nanocomposite powders underwent washing with distilled water and acetone for several times, filtration and drying in vacuum dryer for 2 h at 80°C. The complete fabrication process of the CNT/Ag nanocomposites is illustrated in Figure 1. This process was used for preparing four different CNT/Ag composite powders of 0, 2.5, 5, 10 vol.% of CNTs. The prepared CNT/Ag nanocomposite powders were heat treated at 400°C under hydrogen atmosphere. The prepared powders were characterised using high-resolution scanning electron microscopy (HRSEM), TEM and X-ray Diffractometer.

The produced CNT/Ag nanocomposite powders as well as the pure silver powder underwent spark plasma sintering by using Spark Plasma Sintering System of model Dr. SINTER.LAB at 50 MPa for 1 min. at 550°C under 10^{-3} torr vacuum condition by heating rate up to the sintering temperature was maintained at 100 K/min. The sintering occurred in an uniaxial graphite mould of 12 mm diameter to produce a 2 mm thickness sample for each CNT/Ag nanocomposite. Microstructures characterisations of the produced CNT/Ag nanocomposites were carried out using HRSEM.

Hardness tester of the model Mitutoyo Hardness testing system HM was used for measuring Vickers hardness for the pure silver sample and the related CNT/Ag nanocomposites. The load was selected at 50 gf for testing. The test was repeated five times at different points in each sample. Tensile tests were performed using INSTRON 4206 under a crosshead speed of 0.2 mm/min. Dog-bone shaped sub-size specimens with gage length of 9 mm and width of 2.5 mm based on the ASTM E8M were used for tensile test.

3. Results and discussion

3.1. Synthesis of CNT/silver nanocomposite powders

Multiwall CNTs were functionalised by acid-treatment with sonication to oxidise the surface of the graphene structure by introducing functional groups such as carboxylic, carbonyl and

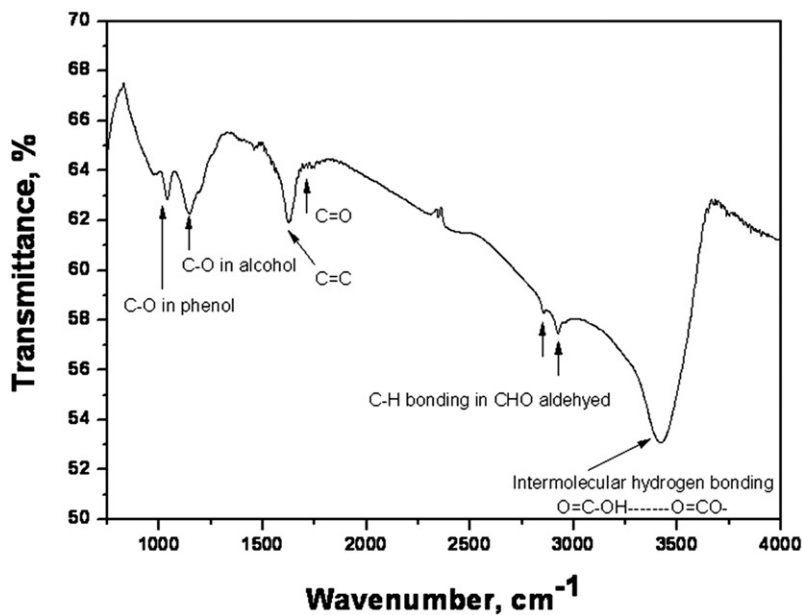


Figure 2. FT-IR chart of the acid-treated CNTs.

hydroxyl groups on the CNTs surfaces. In addition, the functionalisation process enhances the dispersion of the CNTs in the solution by de-capping and the shortening of the CNTs length [23]. The functional groups of the acid-functionalised CNTs were detected by Fourier transform infrared spectroscopy (FT-IR) as shown in Figure 2. The IR chart indicates five kinds of bonding. The first one is the carboxylic group, which is detected by the band at wavenumber 1725 cm^{-1} because of the $\text{C}=\text{O}$ double bond and a broad band at 3421 cm^{-1} because of the intermolecular hydrogen bonding of $\text{O}-\text{H}$ in alcohols and carboxylic acids. The second and the third is the $\text{C}-\text{O}$ group of alcohols and phenols at 1146 cm^{-1} and 1040 cm^{-1} , respectively. In addition a broad band at 3421 cm^{-1} of the intermolecular hydrogen bond of the $\text{O}-\text{H}$ groups is appeared. The fourth functional group is the $\text{C}=\text{C}$ double bond, which was detected by intensive band that appeared at 1625 cm^{-1} indicates the graphene structure of the CNTs. But, the fifth kind of bonding is the $\text{C}-\text{H}$ bonding for the CHO aldehyde group by the two bands at wavenumber 2850 cm^{-1} and 2750 cm^{-1} [24].

The acid-treated CNTs underwent sensitisation in acidic solution of stannous chloride. The sensitised CNTs were coated by silver using alkaline silver nitrate solution and formaldehyde as a reducing agent of silver ion to silver metal.

The silver deposition reaction was completed within 1 h after all the silver ions in the solution were reduced to metallic silver. The chemical bath was used for producing both pure silver powder and coated type CNT/Ag nanocomposite powders. Figure 3(a) shows TEM micrograph of deposited silver powder, which has a particle size of $\sim 40\text{ nm}$.

The most important feature of the process is coating of CNTs with silver metal. Figure 3(b) shows TEM image of activated CNTs by silver. It was observed that CNTs were decorated by silver. But after coating of the activated CNTs by silver, a complete silver layer was deposited on the surface of CNTs as shown in Figure 3(b). It was observed from this microstructure that the silver metal was deposited on the CNT surface in coated type morphology.

The chemical reduction reaction of silver nitrate ($\text{Ag}(\text{NH}_3)_2^+/\text{Ag} + 0.373\text{ V}$) into silver metal by using formaldehyde as a reducing agent have been successfully occurred on the surface of

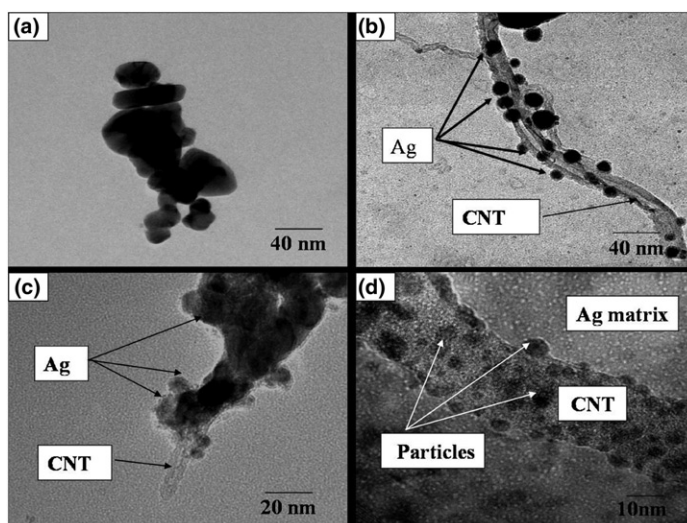


Figure 3. TEM images of (a) the prepared silver powder, (b) the silver activated MWNTs, (c) the silver coated MWNT and (d) the interface between CNTs and Ag matrix.

CNTs. As can be seen, the deposition of metal nanoparticles is achieved via the redox reaction, in which the CNTs act as cathode for metal deposition (Ag) from the reduction of metal ions (Ag^+) in solution. Therefore, the process should allow electroless deposition of metal nanoparticles (Ag) on conductive CNTs.

3.2. Microstructure of sintered CNT/Ag nanocomposites

The produced CNT/Ag nanocomposite powders as well as the pure silver were consolidated into bulk samples by spark plasma sintering, which enable the powders to be sintered by joule heat and spark plasma generated by high-pulsed electric current applied through the compact. Preliminary experiments were being performed to select the optimum conditions of the spark plasma sintering technique. The observations indicate that the shrinkage of the CNT/Ag stopped after 1 min. at 550°C under 50 MPa pressure and 10^{-3} torr vacuum condition. The interface between CNTs and the silver matrix was investigated by TEM as shown in Figure 3(d). It was observed that there are some particles deposited on the surface of CNTs. As illustrated in our previous work, these deposited particles are a kind of intermetallics between the remained tin particles from the sensitisation process, which interact with the silver metal of the matrix by the heating effect during the sintering process [23].

CNT/Ag nanocomposite was also analysed by XRD as shown in Figure 4. Two kinds of peaks, one for pure silver phase and the other for CNTs, are formed. But the peak related to CNTs has some broadening due to formation of the amorphous structure of CNTs by acid treatments.

Figure 5(a) shows a SEM micrograph of the produced pure sintered silver sample by spark plasma sintering. It was observed that the grain size of the pure silver ranged from 100 nm to 200 nm. It can be explained due to the spark plasma sintering technique of the prepared materials occurred in shorter time than the conventional sintering techniques, which inhibit the grain growth in the silver matrix.

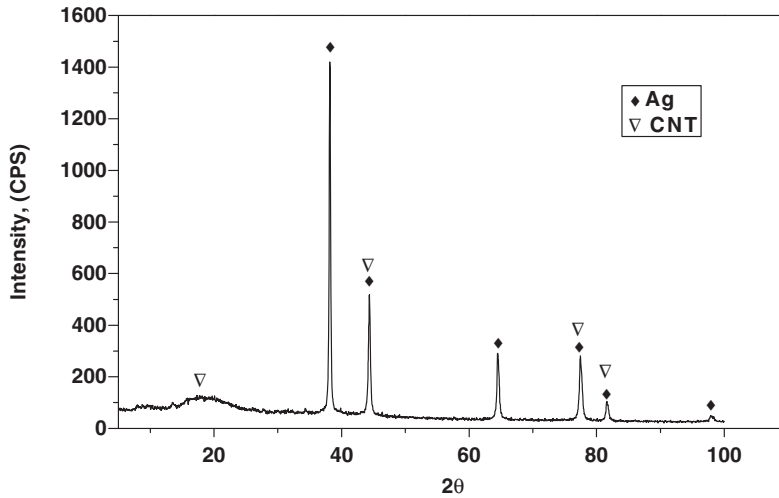


Figure 4. XRD pattern for the produced CNT/Ag nanocomposite powder prepared by chemical reduction in solution.

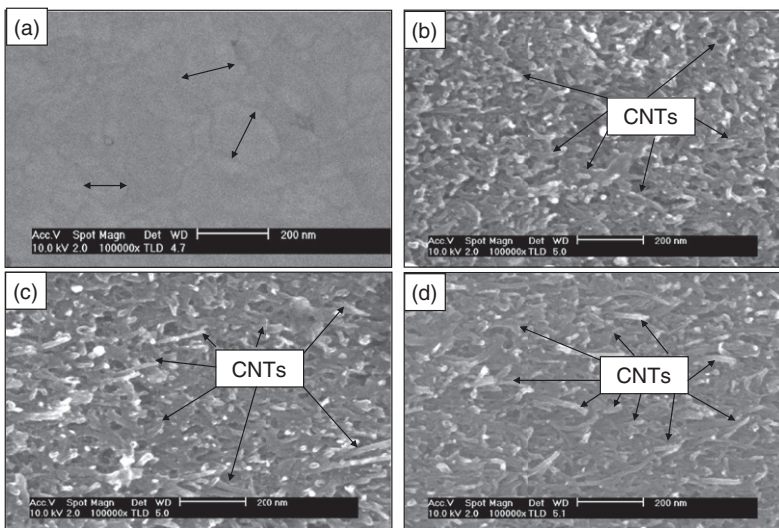


Figure 5. SEM micrographs for sintered CNT/Ag nanocomposites where (a) pure silver (arrows indicate the grain boundaries diameter), (b) 2.5 vol.% CNT/Ag nanocomposite, (c) 5 vol.% CNT/Ag nanocomposite and (d) 10 vol.% CNT/Ag nanocomposite.

Figure 5(b)–(d) show the surface morphology of the etched CNT/Ag nanocomposite samples with 2.5, 5, 10 vol.% of CNTs, respectively. The microstructures of the consolidated CNT/Ag nanocomposites show homogeneous distribution of the CNTs in the silver matrix. In addition, there is no any segregation in silver matrix and fine microstructures without grain coarsening are formed. Furthermore, by increasing the CNTs content, the CNTs volume content was increased and it was observed that by increasing the CNTs volume fraction to 10 vol.% the CNTs can be agglomerated in the silver matrix.

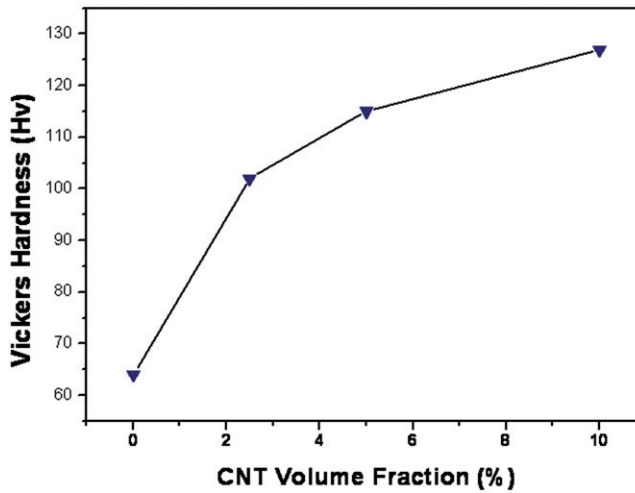


Figure 6. Effect of CNTs volume fraction on the hardness of CNT/Ag nanocomposites.

3.3. Physical and mechanical properties of CNT/Ag nanocomposites

The relative densities of produced CNT/Ag nanocomposites were calculated by the ratio of the measured Archimedes density relative and the calculated densities of the nanocomposite by the role of mixers. It was observed that the relative densities of the CNT/Ag nanocomposites were decreased by increasing the CNT volume fraction from 99.9% in case of (2.5 vol.% CNT)/Ag, which is mainly near to the density of pure silver of 99.91%. But by increasing the CNTs volume, the density decreased to 92.5 in case of (5 vol.% CNT)/Cu and 91.9 in case of 10 vol.% because of to the poor wettability between CNTs and the silver matrix, which enhance the agglomerations of CNTs in silver matrix. In addition, decrease the sinterability of the CNT/Ag nanocomposites. Furthermore, the formation of the tin/silver intermetallics from the remained tin of the sensitisation process on the CNTs surfaces decrease the contact area between the silver matrix and CNTs surface.

The hardness of the CNT/Ag nanocomposites as well as of the pure silver was measured by Vickers hardness test. Figure 6 shows the effect of the CNTs volume fraction on the hardness of the prepared CNT/Ag nanocomposites. It was observed that, the hardness increases by increasing the CNTs volume fraction up to 10 vol.%. In case of (10 vol.% CNT)/Ag nanocomposites, the hardness values reach to maximum at 125 HV, which is about 2.0 times higher than that of pure silver. It is due to the combination between the coating process and the spark plasma, sintering process of the CNT/Ag nanocomposites improve the homogeneous distribution of CNTs in the silver matrix. Therefore, it is confirmed that such remarkable enhancement of hardness by CNTs reinforcements are originated from the high interfacial strength at CNT/Ag interface, the homogeneous distribution of CNTs within silver matrix attained high relative densities. In addition, the intermetallic particles formed between the remained tin from the sensitisation process and the silver matrix increase the hardness of the CNT/Ag nanocomposites [23].

The stress–strain curves are obtained from the tensile test of CNT/Ag nanocomposites as well as the pure silver. The direction of the load is parallel to the compaction direction of the samples. Figure 7 shows stress–strain curve of the produced CNT/Ag nanocomposites with different CNTs volume fraction. The tensile strength of (2.5 vol.% CNT)/Ag nanocomposite is

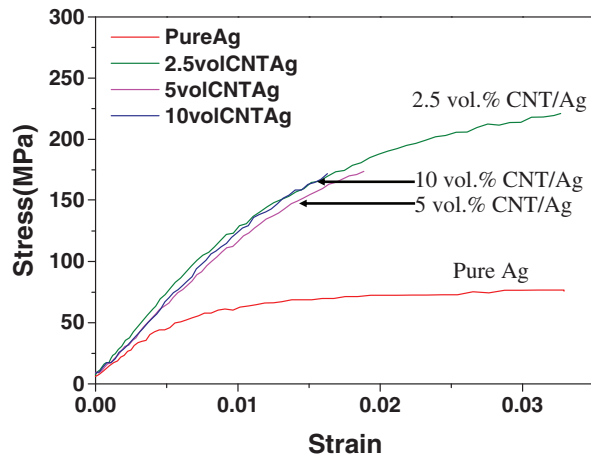


Figure 7. Stress–strain curve of CNT/Ag nanocomposites obtained by tensile test.

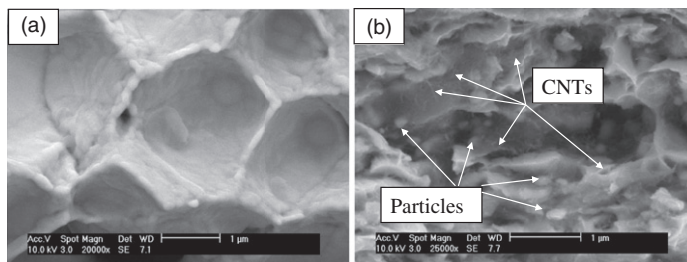


Figure 8. SEM micrographs for the fracture surfaces of (a) pure silver and (b) 10 vol.% CNT/Ag nanocomposite.

measured as 210 MPa, which is approximately three times higher than the corresponding pure sintered silver by spark plasma sintering. However, the tensile strength is decreased to be 2.5 times higher than pure silver in case of 10 vol.% CNT/Ag nanocomposites. The decreasing of the tensile properties by increasing the CNTs volume fraction higher than 2.5 vol.% because of the agglomerations of CNTs in the silver matrix enhances the crack propagations during the tensile strength test. In addition, the formation of tin/silver intermetallics increases the brittleness properties of the CNT/Ag sintered materials. The values of the elongation observed that by increasing the CNTs volume fraction the elongation of the produced CNT/Ag sintered materials were decreased. In case of pure silver, it has 4.1%, which was decreased to 1.1% in case of (2.5 vol.% CNT)/Ag because of the decreasing in the elastic properties of the investigated materials by increasing the CNTs volume fraction higher than 2.5 vol.%. Figures 8(a) and (b) show SEM micrographs to compare between the fracture surface of pure silver and (10 vol.% CNT)/Ag nanocomposite. It was observed that the pure sintered silver has ductile structure but the CNT/Ag nanocomposites have finer grain structure than pure sintered silver with ductile structure. In addition, some of CNTs was pulling out from the silver matrix. It also observed from the fracture surface some tin/silver intermetallic particles were found in the grain boundaries of the silver matrix, which affect on the physical and the mechanical properties of the prepared CNTs/Ag nanocomposites.

4. Summary

CNT/Ag nanocomposites have been fabricated by spark plasma sintering of acid functionalised and silver-coated multiwalled CNTs. The results indicate that the homogeneous distribution of CNTs in the silver matrix is the most critical issues to enhance the physical and mechanical properties of CNT/Ag nanocomposites. The density was decreased, but the hardness was increased by increasing the CNT volume fraction. The tensile strength of the produced CNT/Ag sintered materials was increased by increasing the CNT volume fraction until the CNTs volume fraction reach 10 vol.% the sample was fractured at lower strength value.

References

- [1] J.P. Salvetal, J.M. Bonard, and N.H. Thomson, *Mechanical properties of carbon nanotubes*, Appl. Phys. A 69 (1999), pp. 255–260.
- [2] P.M. Ajayan, *Nanotubes from carbon*, Chem. Rev. 99 (1999), pp. 1787–1799.
- [3] E.T. Thostenson, Z. Ren, and T.W. Chou, *Advances in the science and technology of carbon nanotubes and their composites: A review*, Comput. Sci. Technol. 61 (2001), pp. 1899–1912.
- [4] A.V. Eletsckii, *Carbon nanotubes*, Physics 40 (1997), pp. 899–924.
- [5] S. Iijima, *Single-shell carbon nanotubes of 1-nm diameter*, Nature 363 (1993), pp. 603–605.
- [6] A.B. Sulong and J. Park, *Alignment of multi-walled carbon nanotubes in a polyethylene matrix by extrusion shear flow: Mechanical properties enhancement*, J. Composite. Mat. 45 (2011), pp. 931–941.
- [7] J. Han and C. Gao, *Functionalization of carbon nanotubes and other nanocarbons by azide chemistry*, Nano-Micro Letters 2 (2010), pp. 213–226.
- [8] V.V. Konchits and C.K. Kim, *Electric current passage and interface heating*, Wear 232 (1999), pp. 31–40.
- [9] C.F. Wang, F. Yi, and X.J. Zhang, *Physical properties of short carbon fiber reinforced silver composites*, Acta. Metall. Sin. 7 (1994), pp. 157–160.
- [10] Y. Feng, H. Long Yuan, and M. Zhang, *Fabrication and properties of silver-matrix composites reinforced by carbon nanotubes*, Mat. Character. 55 (2005), pp. 211–218.
- [11] G.S. Paul, *Electrical Contacts: Principles and Applications*, Marcel Dekker, New York, 1999, pp. 628–630.
- [12] Y. Feng, J. Wang, M. Zhang, and Y. Xu, *The influence of pressure on the electrical tribology of carbon nanotube–silver–graphite composite*, J. Mat. Sci. 42 (2007), pp. 9700–9706.
- [13] D.H. He and R. Manory, *A novel electrical contact material with improved self-lubrication for railway current collectors*, Wear 249 (2001), pp. 626–636.
- [14] V.V. Konchits and C.K. Kim, *Electric current page and interface beating*, Wear 232 (1999), pp. 31–40.
- [15] L. Chunyu, R.S. Ruoff, and T.W. Chou, *Modeling of carbon nanotube clamping in tensile tests*, Compos. Sci. Tech. 65 (2005), pp. 2407–2415.
- [16] V.V. Fadin and M.I. Aleutdinova, *Wear resistance of composites for sliding electrical contact from reprocessed bearing steel*, J. Frict. Wear 28 (2007), pp. 4364–4369.
- [17] Z.H. Lü, D.L. Jiang, J.X. Zhang, and Q.L. Lin, *Preparation and properties of multi-wall carbon nanotube/SiC composites by aqueous tape casting*, Sci. China 52 (2009), pp. 132–136.
- [18] A. Fereidoon, M. Rajabpour, and H. Hemmatian, *Investigation of elastic moduli of twisted single wall carbon nanotube based on FEM*, 2011 2nd International Conference on Nanotechnology and Biosensors (ICNB 2011), 28–30 December 2011, Dubai.
- [19] L.A. Montoro, C.A. Luengo, J.M. Rosolen, E. Cazzanelli, and G. Mariotto, *Study of oxygen influence in the production of single-wall carbon nanotubes obtained by arc method using Ni and Y catalyst*, Diam. Relat. Mat. 12 (2003), pp. 846–850.
- [20] Z. Zhongbao and X.U. Shaofan, *Copper-Ti₃SiC₂ composite powder prepared by electroless plating under ultrasonic environment*, Rare Metals 26 (2007), pp. 359–364.
- [21] H. Zhao, G.C. Barber, and J. Liu, *Friction and wear in high speed sliding with and without electrical current*, Wear. 249 (2001), pp. 409–414.
- [22] Y. Sahin and S. Murphy, *The effect of fibre orientation of the dry sliding wear of borsic-reinforced 2014 aluminium alloy*, J. Mat. Sci. 31 (1996), pp. 5399–5407.
- [23] W.M. Daoush, B.K. Lim, C.B. Mo, D.H. Nam, and S.H. Hong, *Electrical and mechanical properties of carbon nanotube reinforced copper nanocomposites fabricated by electroless deposition process*, Mat. Sci. Eng. A 513–514 (2009), pp. 247–253.
- [24] X.H. Chen, C.S. Chen, H.N. Xiao, H.B. Liu, L.P. Zhou, S.L. Li, and G. Zhang, *Dry friction and wear characteristics of nickel/carbon nanotube electroless composite deposits*, Tribol. Int. 39 (2006), pp. 22–28.